Springer

KSME

Journal of Mechanical Science and Technology 30 (7) (2016) 3105~3111
www.springerlink.com/content/1738-494x(Print)/1976-3824(Online)
DOI 10.1007/s12206-016-0619-2

Energy absorption of aluminum alloy thin-walled tubes under axial impact †

Hongtu Sun[1,*], Jian Wang[1], Guozhe Shen[2] and Ping Hu[2]

[1]*School of Transportation, Ludong University, Yantai, 264025, China*
[2]*School of Automotive Engineering, Dalian University of Technology, Dalian, 116024, China*

(Manuscript Received June 10, 2015; Revised February 23, 2016; Accepted March 16, 2016)

Abstract

Aluminum alloys are important technological materials for achieving the lightweight design of automotive structures. Many works have reported on the deformation and energy absorption of thin-walled tubes. Multicorner tubes with extra concave corners in the cross section were presented in this study to improve the energy absorption efficiency of aluminum alloy thin-walled tubes. The axial crushing of square and multicorner thin-walled tubes was simulated with the same cross-sectional perimeter. The method of folding element was applied to predict the crushing behavior of the thin-walled tubes under axial impact. The corners on the cross section were discussed to determine their effect on the energy absorption performance of thin-walled tubes. Results showed that the increasing performance of energy absorption of aluminum alloy thin-walled tubes was caused by the increasing number of corners on the cross section of multicorner tubes. Both the number and size of corners had an important effect on the crushing force efficiency of multicorner tubes. The maximum crushing force efficiency of multicorner tubes was 11.6% higher than that of square tubes with the same material consumption of thin-walled tubes. The multicorner tubes with 12 corners showed better energy absorption performance than the tubes with more than 12 corners; this high number of corners could lead to the small size of corners or unstable deformations. The high energy absorption performance of multicorner tubes prefers increasing the corner number and corner size of adjacent sides at the same time.

Keywords: Aluminum alloy; Axial impact; Deformation; Energy absorption; Thin-walled tubes

1. Introduction

Aluminum alloys are ideal candidate materials for fulfilling the weight reduction demand in the automotive industry [1]. Aluminum alloys are used on automotive structures because of their advantages, including lightweight design and manufacturing flexibility for complex components. An automotive design requires a high performance and a lightweight structure. Longitudinal thin-walled structures on an automotive body usually provide the primary load path for the crushing force and energy absorption during frontal impact [2].

Thin-walled structures are used on kinetic energy absorbers because of their high energy absorption and weight efficiency, particularly under axial crush loads [3]. Numerous works have generally reported the deformation pattern and mechanism of thin-walled tubes under axial crushing for several decades [4-14]. Many studies focus on the experimental and numerical investigations on foam-filled tubes, multicell tubes, hybrid materials, and composite material tubes [15-28]. Wierzbicki and Abramowicz presented significant theoretical analyses and research into the crushing behavior of thin-walled square tubes [7]. A deformation occurs around the corners of tubes to dissipate most of the energy. Therefore, the number of corners at the cross section of thin-walled tubes has an important effect on energy absorption efficiency [15]. The behavior of square thin-walled aluminum alloy tubes subjected to axial loading was studied using static and dynamic tests [16]. The dynamic mean force, which is significantly higher than the corresponding static force, indicates a strong inertia effect with respect to the axial displacement. The folding deformation characteristics of aluminum alloy thin-walled polygonal section tubes subjected to dynamic axial impacts were investigated using numerical simulation [17]. The increase in the number of walls has a direct effect on the mean crushing force and the permanent displacement parameters. The S-shape front rails with materials of aluminum alloy and steel are introduced to reduce the peak impact force while increasing the total absorption energy for lightweight automotive structures [18]. The fracture possibility of thin-walled tubes was analyzed under axial crushing [19]. The fracture of thin-walled tubes more likely occurs on the edge than on other positions. The mean crushing forces were calculated for single, double, and triple cells under quasistatic axial loading for energy absorption [20]. Innovative multicell structures with an additional folding element at each corner of the square column

*Corresponding author. Tel.: +86 535 6652251, Fax.: +86 535 6652251
E-mail address: hongtusun@163.com
† Recommended by Associate Editor Byeng Dong Youn

were proposed to improve the specific energy absorption over the conventional square tubes [21]. A theoretical solution to square multicell tubes was introduced to show the increasing energy absorption efficiency of multicell square tubes [22]. The strategy to improve energy absorption efficiency of thin-walled tubes was proposed by introducing an extra nonconvex corner in the cross section [23].

In this research, the multicorner tubes with extra concave corners in the cross section were presented to analyze the energy absorption efficiency of aluminum alloy thin-walled tubes. The identical results of the simulation and theoretical prediction using the folding element method indicated the validity of the finite element model of aluminum alloy thin-walled tubes. The energy absorption of the multicorner tubes with different cross sections was investigated using numerical simulation. The design of multicorner tubes with extra concave corners presents an effective structure to improve the energy absorption performance of thin-walled tubes. The results of this research can provide a valuable design criterion for the manufacturing and application of thin-walled structures.

2. Theoretical prediction

Crushing forces during folding deformations are the most important parameters for the energy absorption of thin-walled tubes. The mean crushing force F_m is defined by

$$F_m = \frac{\int F d\delta}{\delta_p}, \tag{1}$$

where F is the crushing force during the displacement δ, and δ_p is the permanent displacement. The specific energy absorption E_s is defined by

$$E_s = \frac{\int F d\delta}{m}, \tag{2}$$

where m is the mass of the thin-walled tube. The crushing force efficiency η_F is defined by

$$\eta_F = \frac{F_m}{F_p}, \tag{3}$$

where F_p is the peak crushing force during the deformation. A high crushing force efficiency indicates a good crushing force consistency and energy absorption.

The mean crushing force can be predicted according to the plastic flow stress of the material, wall thickness, and sectional width using the folding element method, which was developed by Wierzbicki and Abramowicz [7]. The mean crushing force F_m of the square tubes for a rigid plastic material [8] is expressed as

$$F_m = 13.06\sigma_0 b^{1/3} t^{5/3}, \tag{4}$$

where σ_0 is the plastic flow stress of the material, t is the wall thickness, and b is the sectional width.

Two types of basic folding elements are involved in the folding element method to analyze thin-walled tubes under axial crushing. A kinematical approach is applied for the precise energy dissipation contribution of the extensional and bending deformation in the method. Basic elements are used to predict the axial collapse behavior of square tubes [5-8]. The energy absorption of a basic folding element for each corner is

$$E = M_0(16I_1Hr/t + 2\pi l_i + 4I_3H^2/r), \tag{5}$$

where H is the half folding wavelength, I_1 and I_3 are defined by the angle between two adjacent plates, l_i is the flange length around the corner, and r is the radius of the toroidal shell element in the kinematically admissible velocity field [8]. The energy balance equation is expressed as

$$F_m 2H / M_0 = \sum_{i=1}^{N}(16I_1Hr/t + 2\pi l_i + 4I_3H^2/r), \tag{6}$$

where N is the number of corners in the cross section of tubes. When minimized, the mean crushing force presents the following with respect to parameter H:

$$\partial F_m / \partial H = 0, \quad \partial F_m / \partial r = 0. \tag{7}$$

The parameters H and r are solved using Eq. (7). The mean crushing force F_m can be solved by substituting H and r back into Eq. (6).

If the effect of dynamic crushing is considered, then the dynamic amplification factor D_a is introduced as dynamic effects, which present the dynamic crushing effect of sectional width, wall thickness, material density, flow stress and impacting velocity of thin-walled tubes. Then, the dynamic mean crushing force F_{dm} is expressed as

$$F_{dm} = D_a F_m. \tag{8}$$

The dynamic amplification factor of aluminum alloy AA6060-T4, which ranges from 1.3 to 1.6, was proposed by Langseth and Hopperstad [16]. The dynamic amplification factor of D_a is selected as 1.3 for simplicity in this research.

3. Finite element model

The schematic diagram of the models is shown in Fig. 1. The materials, boundary conditions, and load conditions of all the models were identical. The boundary constraints were similar for all the tube walls, with the lower end fixed and the top end attached to a rigid wall with an initial axial impacting velocity of v = 10 m/s for all the models. The rigid wall was

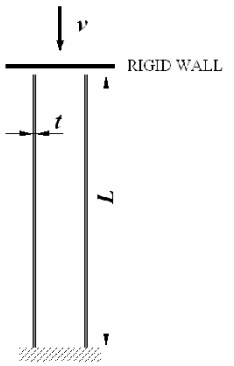

Fig. 1. Schematic diagram of the models.

modeled using one degree of freedom with the impacting direction of the z axis. The total simulated impact mass was constant at 55.9 kg for all the model configurations.

All the thin-walled tubes were modeled with varying wall thicknesses t ranging from 1 mm to 3 mm and with a length L of 400 mm. The sectional width b for the unified section square tubes was 80 mm.

All the thin-walled tubes were modeled using Belytschko-Tsay four-node shell elements with nine integration points through the thickness and one integration point in the element plane. The mesh size of 4 mm × 4 mm for all tubes was adopted after the simulations of optimal mesh density for accurate deformation process and solution time.

The tube material was aluminum alloy AA6060 with Young's modulus E of 68.21 GPa, Poisson's ratio v of 0.3, yield strength σ_y of 190 MPa, ultimate strength σ_u of 213 MPa, and ultimate elongation ε_u of 0.1. The modified piecewise linear plasticity model (Material type #24) was adopted to describe the material behavior of the tubes. This material model provided a multilinear elastic plastic material option that allowed stress and strain curve input and strain rate while introducing the enhanced failure criteria. The failure criteria were based on the plastic strain, which was 0.1 in the numerical simulation.

A single surface contact algorithm was selected to simulate the axial crushing deformation of the tubes. This contact type used nodal normal projection and prevented elements from penetrating the wall surfaces during the axial collapsing movement of the tube. The finite element models were performed using the dynamic nonlinear explicit finite element code ANSYS/LS-DYNA.

4. Numerical simulation results

4.1 Square tubes

Progressive folding deformations were the main folding mode for all aluminum alloy thin-walled tubes. An increased number of folding deformations indicated highly severe deformations of thin-walled tubes. These deformations led to high energy absorption efficiency. The typical folding deformation plots of thin-walled tubes are shown in Fig. 2.

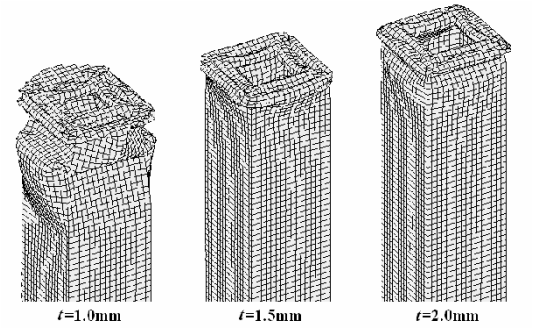

Fig. 2. Folding deformations of square thin-walled tubes.

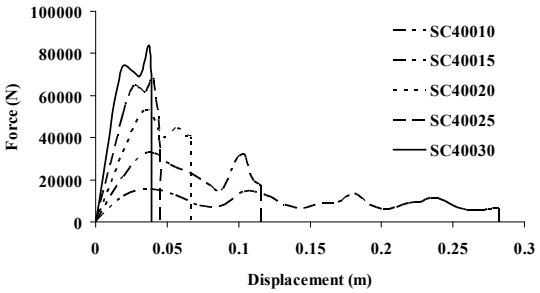

Fig. 3. Crushing force curves of square thin-walled tubes.

The folding deformations consisted of the symmetric collapse modes and extensional collapse mode for the thin-walled tube of t = 1 mm. However, extensional collapse modes were the main collapse mode as the wall thickness increased. The deformations with t = 2.5 mm and t = 3 mm, which were not presented in the figure, were approximately the same as those of t = 2 mm.

The crushing forces with displacements are shown in Fig. 3. The crushing forces fluctuated around the mean values at the effective crushing length. The number of the force waves was the number of folding deformations. The corners indicated the constraints during the deformation. The progressive buckling deformations of the square tubes were caused by the few corners on the cross section, leading to a less critical local buckling load than the critical global buckling load.

The simulation results are listed with the different thicknesses of thin-walled tubes in Table 1. The mass m was calculated according to the width, thickness, and density of the tube. The increase in thickness of the thin-walled tubes had a direct effect on the crushing force and permanent displacement. The increase of the mean crushing force F_m and the peak crushing force F_p was obvious with the increase in tube thickness. However, the permanent displacement δ_p appeared on the opposite situation. The crushing force efficiency η_F also increased with the increase in wall thickness. This scenario indicated the high performance of energy absorption. However, the specific energy absorption E_s decreased because of the increased mass of the thin-walled tubes.

The square thin-walled tubes showed similar folding modes as the impacting energy increased. The energy absorption

Table 1. Simulation results of square thin-walled tubes.

Index	t (mm)	F_m (kN)	F_p (kN)	δ_p (m)	m (kg)	E_s (kJ/kg)	η_F (%)
SC40010	1.0	9.6	14.6	0.282	0.356	7.9	65.8
SC40015	1.5	24.3	33.2	0.115	0.534	5.2	73.3
SC40020	2.0	41.8	53.3	0.067	0.712	3.9	78.4
SC40025	2.5	62.2	68.1	0.045	0.890	3.1	81.8
SC40030	3.0	71.8	83.8	0.039	1.068	2.6	85.7

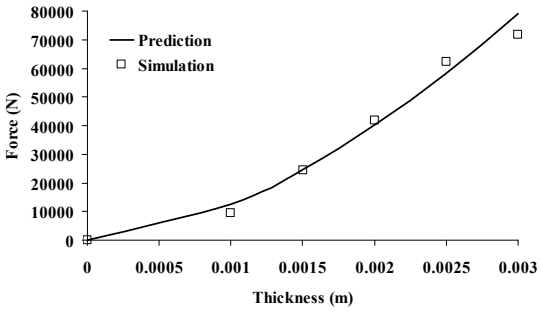

Fig. 4. Mean crushing forces of square tubes predicted using theoretical solutions and numerical simulations.

performance of the thick wall for aluminum alloy tubes was potentially better than that of the thin wall because of the increasing crushing force efficiency. However, the high peak crushing force of the thick square tubes for an automotive body with aluminum alloy tubes might lead to increased risks of injury to passengers.

The mean crushing forces of square tubes could be predicted using the folding element method with consideration of the dynamic effect, as shown in Fig. 4.

The mean crushing forces of the simulation results were consistent with those predicted using the theoretical method. The simulation results of the mean crushing forces were also verified by comparing them with the experimental test results of the mean crushing forces [16, 17].

The two groups of experimental test results [16] were selected to compare the numerical simulations with the wall thicknesses of 2 and 2.5 mm. The parameters of the simulations were close to those of the experimental test. Fig. 5 shows that the average experimental result of the mean crushing forces was 40.1 kN for the seven specimens with the wall thickness of 2 mm. The percentage difference of the simulation was 4.24%. The average experimental value of the mean crushing forces was 64.7 kN for the seven specimens with the wall thickness of 2.5 mm. The percentage difference of the simulation was 3.86%. The reasonable and stable numerical simulation models also provided the possibility of researching other sectional shape tubes.

4.2 Multicorner concave tubes

Energy absorption is the main issue for the majority of studies on thin-walled tubes. Deformations around the corners that

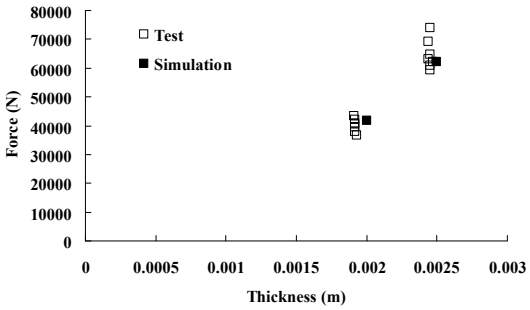

Fig. 5. Mean forces of square tubes with experimental tests and numerical simulation.

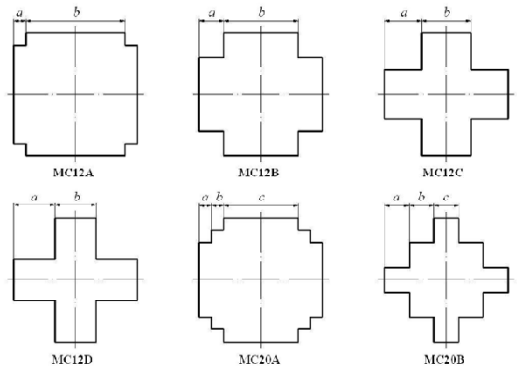

Fig. 6. Cross-sectional dimensions of multicorner concave tubes.

dissipate the most crushing energy are supposed to distribute materials to improve energy absorption efficiency [20]. However, the corners of the adjacent side at some extent of the angle present high performance for energy absorption. The corners of the cross section of a regular polygon are limited because of the optimal angle range. Thus, the energy absorption efficiency cannot be adequately improved only by increasing the number of corners for regular polygon tubes [24].

Multicell structures potentially improve energy absorption efficiency by introducing internal webs in the cross section of thin-walled tubes. However, the complex structure and manufacturing technology of multicell structures hinder the application of multicell structures on the complicated structures of automotive structures. A new type of concave multicorner tubes is proposed to improve energy absorption efficiency [23]. Fig. 6 shows that the multicorner tubes have many types for the symmetrical cross section.

The feature of this kind of multicorner tube is that the perimeters of the cross-sectional shape are all the same as those of the corresponding square tube regardless of the number of corners. This feature also means that the mass for all types of multicorner tubes is consistent with the same length and thickness of tubes.

The multicorner cross section varies with the lengths of *a*, *b*, and *c* around the corners in Fig. 6. One type of a multicorner cross section, such as 12 corners (i.e., MC12D) and 20 corners (i.e., MC20B) with the same lengths of *a*, *b*, or *c*, is shown in

Table 2. Geometric dimensions of multicorner concave tubes.

Index	a (mm)	b (mm)	c (mm)	Corners
MC12A	10	60	-	12
MC12B	20	40	-	12
MC12C	30	20	-	12
MC12D	26.7	26.7	-	12
MC20A	8	8	48	20
MC20B	16	16	16	20

Fig. 6. The other type of a multicorner cross section is the one with different lengths of *a*, *b*, or *c*. This type can shape various types of cross sections with many corners. Fig. 6 shows several regular concave multicorner cross sections (i.e., MC12A, MC12B, MC12C and MC20A), which are selected as the energy absorption structure in this research for appropriate manufacturability and structure. The geometric dimensions of all the studied multicorner shapes are listed in Table 2.

All the multicorner thin-walled tubes of the varied cross sections are simulated with the same model parameters of the aforementioned square thin-walled tubes. Then, the mass of all the multicorner tubes was 0.356 kg. All these tubes have the same thickness t of 1 mm and the length L of 400 mm.

The deformations of the multicorner tubes are shown in Fig. 7. The multicorner tubes of MC12A, MC12B, MC12C, MC12D, and MC20A present the extensional collapse mode for high energy absorption performance. The increased number of corners improves the local buckling capacity because of the increased constraints on the wall.

However, the multicorner tube of MC20B performs a different collapse mode. Fig. 7 shows that the earlier toroidal deformation with the later Euler deformation has a negative effect on the energy absorption of the thin-walled tubes. The tendency of this deformation increases with the increase in wall thickness. The energy absorption of MC20B is unstable with varied wall thickness. The thin-walled tubes deform progressively and stably when the critical local buckling loads are lower than the critical global buckling loads. The critical local and global buckling loads increase while the thicknesses of walls increase. The increasing velocity of the critical local buckling loads is higher than that of the critical global buckling load because of the increased number of corners. The unstable deformations of MC20B are present when the critical local buckling loads are higher than the critical global buckling loads.

The crushing forces with the displacements are shown in Fig. 8. The crushing forces are close for the similar cross-sectional multicorner tubes, such as MC12A and MC20A, MC12B and MC20B, and MC12C and MC12D.

The simulation results of the multicorner tubes are listed in Table 3. The deformations of the multicorner tubes are less than those of the square tubes because of the high crushing forces of the former. The mean crushing force F_m and peak crushing force F_p of the tubes with 12 corners are higher than

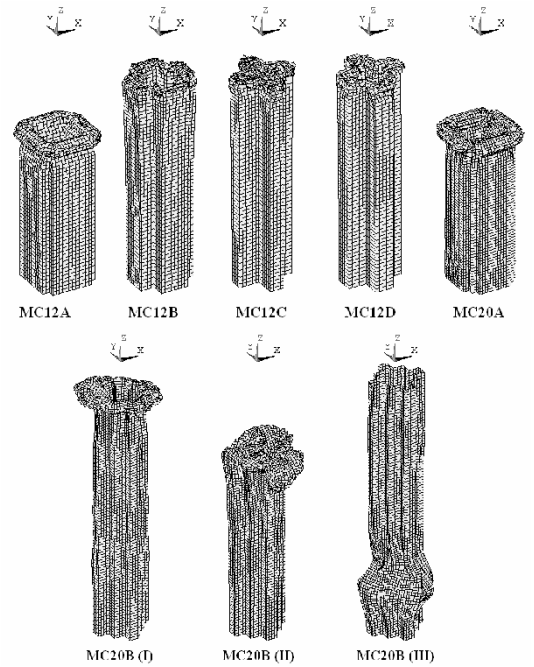

Fig. 7. Folding deformation of multicorner concave tubes.

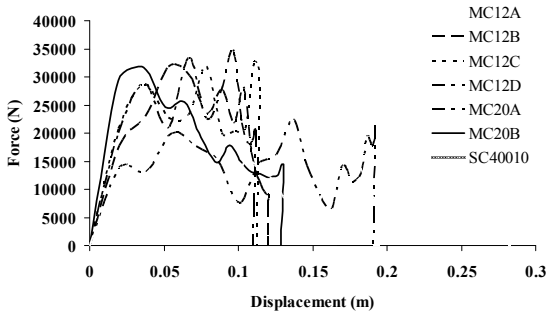

Fig. 8. Crushing force curves of multicorner concave tubes.

those of the square tube. The crushing force efficiency of MC12D is 77.4%, which is 11.6% higher than that of the square tube of SC40010. The increase of the crushing force efficiency η_F indicates that the high performance of energy absorption of multicorner tubes is caused by the increased number of corners. The high number of corners improves the folding capacity of the tube. The difference among the multicorner tubes of MC12A, MC12B, MC12C, and MC12D is the length of the corner adjacent side, which plays an important role in crushing force efficiency.

The corners with a small size have a minimal effect on the performance of energy absorption. These corners cannot adequately improve the performance of energy absorption. This inadequate energy absorption performance is similar to that of the square tube, despite the increased number of corners at the tubes of MC12A and MC20A.

Table 3 shows the multicorner tubes of MC12C and MC12D. The close adjacent sides of the 12 corners show maximum η_F. A slightly increased η_F is shown at the tube of

Table 3. Simulation results of multicorner concave tubes.

Index	F_m (kN)	F_p (kN)	δ_p (m)	E_s (kJ/kg)	η_F (%)
SC40010	9.6	14.6	0.282	7.9	65.8
MC12A	14.3	21.4	0.196	7.9	66.8
MC12B	23.3	31.8	0.12	7.9	73.4
MC12C	24.6	31.9	0.114	7.9	77.0
MC12D	25	33.3	0.112	7.9	77.4
MC20A	14.6	22.1	0.192	7.9	66.1
MC20B	21.5	31.7	0.13	7.9	67.9

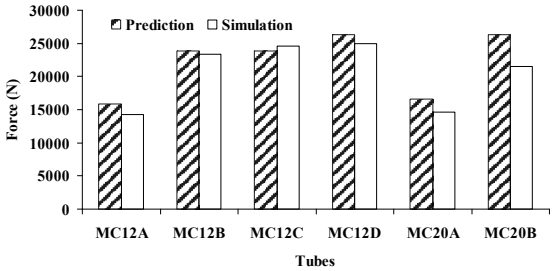

Fig. 9. Mean forces of multicorner concave tubes predicted by theoretical solutions and numerical simulations.

MC20B because of the large size of the corners. However, the η_F of the tube with 20 corners is lower than that of the tube with 12 corners. This finding indicates that the unstable flower or drum deformations can develop to Euler deformation, which leads to the decreasing performance of energy absorption.

The mean crushing forces of multicorner tubes can also be predicted as square tubes. The effect of the corner size is considered for the theoretical prediction. Fig. 9 shows that the results of the simulation and prediction are close, except for MC20B. This different result is caused by the collapse mode of MC20B, which is not considered by the theoretical method.

The length variation of the multicorner tubes is investigated for its effect on the energy absorption performance. The tube lengths L of 300 and 500 mm are also selected for each multicorner tube. The crushing behaviors of the multicorner tubes of L = 300 mm and L = 500 mm are similar to that of the multicorner tubes of L = 400 mm in the effective crushing displacements for the majority of the multicorner tubes. However, the unstable deformations of MC20B are present as the length of the tubes increases, thereby leading to the decrease in critical global buckling load. The tendency of Euler deformations for multicorner tubes is more obvious than that for square tubes, which have few constraints at the corners.

5. Conclusions

The increasing energy absorption performance of multicorner tubes was caused by the increased number of corners on the cross section of thin-walled tubes. Both the number and size of corners had an important effect on the crushing force efficiency of multicorner tubes. The maximum crushing force efficiency of multicorner tubes was 11.6% higher than that of square tubes with the same material consumption of thin-walled tubes. The multicorner tubes with 12 corners showed better energy absorption performance than the tubes with an increased number of corners despite the same cross-sectional perimeter and mass of tubes. The increased number of corners could lead to the small size of corners or unstable deformations. The high energy absorption performance of multicorner tubes prefers increasing the corner number and corner size of adjacent sides at the same time.

Acknowledgment

This project is supported by the National Natural Science Foundation of China (Grant Nos. 10932003 and 51401100).

References

[1] S. Toros, F. Ozturk and I. Kacar, Review of warm forming of aluminum-magnesium alloys, *Journal of Materials Processing Technology*, 207 (2008) 1-12.

[2] W. S. Miller, L. Zhuang, J. Bottema, A. J. Wittebrood, P. D. Semt, A. Haszler and A. Vieregge, Recent development in aluminum alloys for the automotive industry, *Material Science and Engineering*, A280 (2000) 37-49.

[3] G. X. Lu and T. X. Yu, *Energy absorption of structures and materials*, Woodhead Publishing Ltd., Cambridge (2003).

[4] J. M. Alexander, An approximate analysis of the collapse of thin cylindrical shells under axial load, *Quarterly Journal of Mechanics and Applied Mathematics*, 13 (1960) 10-15.

[5] W. Abramowicz and N. Jones, Dynamic axial crushing of square tubes, *International Journal of Impact Engineering*, 2 (1984) 179-208.

[6] W. Abramowicz and N. Jones, Dynamic axial crushing of circular tubes, *International Journal of Impact Engineering*, 2 (1984) 263-281.

[7] T. Wierzbicki and W. Abramowicz, On the crushing mechanics of thin-walled structures, *Journal of Applied Mechanics*, 50 (1983) 727-734.

[8] W. Abramowicz and N. Jones, Dynamic progressive buckling of circular and square tubes, *International Journal of Impact Engineering*, 4 (4) (1986) 243-270.

[9] W. Abramowicz, Thin-walled structures as impact energy absorbers, *Thin-Walled Structures*, 41 (2003) 91-107.

[10] W. Abramowicz and T. Wierzbicki, Axial crushing of multi-corner sheet metal columns, *Journal of Applied Mechanics*, 56 (1989) 113-120.

[11] L. Sun, D. Leng, J. Sun, Y. Lin and D. Wang, An equivalent stiffness (ES) method for initial design of tube-based energy absorbers under lateral quasi-static compression, *Journal of Mechanical Science and Technology*, 29 (2) (2015) 637-646.

[12] R. Alipour, A. Farokhi Nejad and S. Izman, The reliability of finite element analysis results of the low impact test in

predicting the energy absorption performance of thin-walled structures, *Journal of Mechanical Science and Technology*, 29 (5) (2015) 2035-2045.

[13] K. W. Hou, J. L. Yang, H. Liu and Y. X. Sun, Energy absorption behavior of metallic staggered double-sine-wave tubes under axial crushing, *Journal of Mechanical Science and Technology*, 29 (6) (2015) 2439-2449.

[14] S. Choi and K.-Y. Jhang, Influence of repetitive pulsed laser irradiation on the surface characteristics of an aluminum alloy in the melting regime, *Journal of Mechanical Science and Technology*, 29 (1) (2015) 335-340.

[15] S. P. Santosa, T. Wierzbicki, A. G. Hanssen and M. Langseth, Experimental and numerical studies of foam-filled sections, *International Journal of Impact Engineering*, 24 (2000) 509-534.

[16] M. Langseth and O. S. Hopperstad, Static and dynamic axial crushing of square thin-Walled aluminum extrusions, *International Journal of Impact Engineering*, 18 (1996) 949-968.

[17] A. Rossi, Z. Fawaz and K. Behdinan, Numerical simulation of the axial collapse of thin-walled polygonal section tubes, *Thin-Walled Structures*, 43 (2005) 1646-1661.

[18] Y. J. Zhou, F. C. Lan and J. Q. Chen, Crashworthiness research on S-shape front rails made of steel-aluminum hybrid materials, *Thin-Walled Structures*, 49 (2011) 291-297.

[19] G. Y. Gu, Y. Xia and Q. Zhou, On the fracture possibility of thin-walled tubes under axial crushing, *Thin-Walled Structures*, 55 (2012) 85-95.

[20] W. G. Chen and T. Wierzbicki, Relative merits of single-cell, multi-cell and foam-filled thin-walled structures in energy absorption, *Thin-Walled Structures*, 39 (4) (2001) 287-306.

[21] H. S. Kim, New extruded multi-cell aluminum profile for maximum crash energy absorption and weight efficiency, *Thin-Walled Structures*, 40 (4) (2002) 311-327.

[22] X. Zhang, G. D. Cheng and H. Zhang, Theoretical prediction and numerical simulation of multi-cell square thin-walled structures, *Thin-Walled Structures*, 44 (11) (2006) 1185-1191.

[23] Z. L. Tang, S. T. Liu and Z. H. Zhang, Energy absorption properties of non-convex multi-corner thin-walled columns, *Thin-Walled Structures*, 51 (2012) 112-120.

[24] M. Yamashita, M. Gotoh and Y. Sawairi, Axial crush of hollow cylindrical structures with carious polygonal cross-sections numerical simulation and experiment, *Journal of Materials Processing Technology*, 140 (2003) 59-64.

[25] P. Paruka and W. A. Siswanto, Axial impact performance of aluminum thin cylindrical tube, *Applied Mechanics and Materials*, 315 (2013) 1-5.

[26] B. Y. Kim, C. M. Jeong, S. W. Kim and M. W. Suh, A study to maximize the crash energy absorption efficiency with the limits of crash space, *Journal of Mechanical Science and Technology*, 26 (4) (2012) 1073-1078.

[27] J. Yoon, Y. Lee and H. Huh, Investigation of deformation and collapse mechanism for magnesium tube in axial crushing test, *Journal of Mechanical Science and Technology*, 27 (10) (2013) 2917-2921.

[28] P. Paruka, W. A. Siswanto, M. A. Maleque and M. K. M Shah, Crashworthy capacity of a hybridized epoxy-glass fiber aluminum columnar tube using repeated axial resistive force, *Journal of Mechanical Science and Technology*, 29 (5) (2015) 1941-1953.

Hongtu Sun, born in 1977, is currently an associate professor of the School of Transportation at Ludong University, Yantai, China. He received his Ph.D. in Vehicle Engineering (2009) at Dalian University of Technology, Dalian, China. His research interests include lightweight design and safety of vehicle body.